Available online at www.sciencedirect.com
ScienceDirect
Applied Radiation and Isotopes 66 (2008) 545–551
Applied Radiation and Isotopes
www.elsevier.com/locate/apradiso

Production of the therapeutic radionuclides ^{193m}Pt and ^{195m}Pt with high specific activity via α-particle-induced reactions on ^{192}Os

K. Hilgers, H.H. Coenen, S.M. Qaim*

Institut für Nuklearchemie, Forschungszentrum Jülich GmbH, D-52425 Jülich, Germany

Received 7 July 2007; received in revised form 18 October 2007; accepted 22 October 2007

Abstract

For the production of therapy-relevant radionuclides ^{193m}Pt ($T_{1/2} = 4.33$ d) and ^{195m}Pt ($T_{1/2} = 4.03$ d) with a high specific activity, the ^{192}Os(α,n)^{195m}Pt and ^{192}Os(α,3n)^{193m}Pt nuclear reactions were investigated for the first time from their respective thresholds up to 28 MeV. Thin samples of enriched ^{192}Os were prepared by electrodeposition on Ni, and the conventional stacked-foil technique was used for cross-section measurements. The calculated thick target yields were found to be 0.013 MBq/μA h for the ^{192}Os(α,n)^{195m}Pt reaction in the energy range of $E_\alpha = 24 \rightarrow 18$ MeV, and 0.25 MBq/μA h for the ^{192}Os(α,3n)^{193m}Pt reaction in the energy range of $E_\alpha = 28 \rightarrow 24$ MeV. The two radionuclides could not be detected in the interactions of ^{3}He particles with ^{192}Os. A production method involving high-current α-particle irradiation of enriched ^{192}Os and efficient chemical separation of radioplatinum was developed. Batch yields of about 1 MBq ^{195m}Pt and 8.7 MBq ^{193m}Pt were achieved. Compared to the reactor production these batch yields are very low, but the ^{192}Os(α,n)^{195m}Pt and ^{192}Os(α,3n)^{193m}Pt reactions are superior with respect to the specific activity of the products which is higher by two orders of magnitude.

Keywords: Platinum-193m; Platinum-195m; α-Particle irradiation; Osmium-192; Cross-section; Excitation function; High current irradiation; Chemical separation; Quality control; Internal radiotherapy

1. Introduction

Internal radiotherapy can provide high radiation doses to the target tissue without or only with a small amount of damage done to the healthy tissue, provided a suitable radionuclide is used in combination with a specific chemical vehicle. Thus, this form of radiotherapy promises to be a more gentle method of fighting illnesses like cancer. A suitable radionuclide for internal therapy shows a high-intensity radiation with a high linear energy transfer and a 10–20% abundance of about a 150–200 keV γ-ray. The half-life must be in the order of about 3–8 d to achieve a suitable radiation dose in the target tissue. Thus, the radionuclides fulfilling these requirements emit α^- or β^- particles, or conversion and Auger electrons (Hoefnagel, 1991; Qaim, 2001).

In recent years, low-energy electron emitters have been gaining considerable significance (Mariani et al., 2000). Two such nuclides are ^{193m}Pt ($T_{1/2} = 4.33$ d, IT = 100%, no γ-radiation) and ^{195m}Pt ($T_{1/2} = 4.03$ d, IT = 100%, $E_\gamma = 98.9$ keV, $I_\gamma = 11.4\%$). Both isomeric states deexcite by internal transition and emit conversion electrons. They also emit high-intensity Auger electrons. According to Mariani et al. (2000), for example, the radionuclide ^{195m}Pt exhibits a very high Auger electron yield, with an average of 33 electrons emitted per decay versus 21 electrons for ^{125}I and 8 electrons for ^{111}In, the two commonly used radionuclides in endoradiotherapy at present. Similarly, ^{193m}Pt exhibits a yield of 26 Auger electrons per decay (Azure et al., 1992).

The potential therapeutic applications of ^{193m}Pt and ^{195m}Pt are not only due to their suitable decay properties but also because platinum complexes (like *cis*-platin and others) are used in chemotherapy. They are potent antitumour agents and are therefore very interesting. In order to avoid the side effects of chemotherapy, it is

*Corresponding author. Tel.: +49 2461 613282; fax: +49 2461 612535.
E-mail address: s.m.qaim@fz-juelich.de (S.M. Qaim).

0969-8043/$ - see front matter © 2007 Elsevier Ltd. All rights reserved.
doi:10.1016/j.apradiso.2007.10.009

advisable to use these radionuclides in the same or similar chemical complexes with a high specific activity.

Several compounds have been labelled with ^{195m}Pt (Hoeschele et al., 1982; Akaboshi, 2003). However, since the ^{195m}Pt used was produced in a nuclear reactor via the ^{194}Pt(n,γ) process, the product was carrier-added. The situation is aggravated by the fact that the cross-section of the ^{194}Pt(n,γ)^{195m}Pt reaction is small (0.09 b) compared to the ^{195m}Pt(n,γ)^{196}Pt reaction burn-up cross-section of 13,000 b (Hoeschele et al., 1982). The specific activity could be improved by irradiation of enriched ^{194}Pt in a high-flux reactor. Nonetheless, the final product achieved is still not of high specific activity (Hoeschele et al., 1982; Akaboshi, 2003). The situation with ^{193m}Pt is similar. It was also produced in a nuclear reactor via the ^{192}Pt(n,γ) reaction. The specific activity achieved was 10–40 times higher than in the case of ^{195m}Pt (Azure et al., 1992), but further efforts are needed to obtain a still higher specific activity.

With a view to enhancing the specific activity, the production of these nuclides was investigated in charged-particle-induced reactions. As can be seen from the nuclear properties, both the platinum nuclides are isomeric states with a high spin of $13/2^+$. Charged particles with a high angular momentum thus ought to be more suitable to produce these nuclides. Some attempts have been made to produce Pt radionuclides in irradiations of ^{nat}Os with α-particles (Tinker et al., 1991; Groppi et al., 2001). However, to date neither ^{195m}Pt nor ^{193m}Pt has been obtained in a no-carrier-added form in a radionuclidically pure state. In the present work, we investigated the formation of ^{193m}Pt and ^{195m}Pt in α- and ^{3}He-particle irradiations of enriched ^{192}Os. This work gives the first systematic cross-section data for the ^{192}Os(α,n)^{195m}Pt and ^{192}Os(α,3n)^{193m}Pt reactions up to 28 MeV.

2. Cross-section data

2.1. Experimental

The conventional stacked-foil technique was used for cross-section measurements. Some of the salient features are given below.

2.1.1. Sample preparation

Thin osmium samples were prepared by electrolytic deposition of enriched ^{192}Os (supplied by Chemotrade; chemical purity: 99.9 + %, isotopic composition: 84.5% ^{192}Os, 15.2% ^{190}Os, 0.3% ^{189}Os) on 25 μm thick Ni foils (99.9% pure, Goodfellow) from an alkaline solution (Fresenius and Jander, 1951; Chakrabarty et al., 2001). To prepare the electrolytic solution, osmium powder was dissolved in concentrated nitric acid by heating, and the OsO_4 formed was distilled into an alkaline solution of KOH or NaOH. About 1.5 mL of the solution was then transferred to the electrolytic cell (cf. Mushtaq and Qaim, 1990). The Ni backing foil served as a cathode and a rotating Pt-anode wire as the anode. For electroplating, a potential of 6–10 V and a current of about 0.9 A were applied for 1 h. The electrolytic deposit of metallic osmium had a mass between 1 and 4 mg, which was determined by weighing. The uniformity of the deposit was checked using a microscope. Also the absence of all oxides, which are coloured, could be confirmed. Thereafter, the osmium deposit was covered by a 10 μm thick Al foil. The sample was then ready for irradiation. In a few cases, a check of the chemical purity was also done via proton activation analysis. No positron-emitting activity was detected, i.e. ^{13}N ($T_{1/2} = 9.96$ min) or ^{18}F ($T_{1/2} = 109.7$ min), which would have been formed via the ^{16}O(p,α)^{13}N and ^{18}O(p,n)^{18}F reactions, respectively, if oxygen impurity had been present.

2.1.2. Irradiations and beam flux monitoring

Irradiations were carried out at the compact cyclotron CV 28 of the Forschungszentrum Jülich GmbH with a primary α-particle energy of 28 MeV and primary ^{3}He-particle energies of 25 and 36 MeV. Several stacks consisting of a few ^{192}Os samples and thin Ti and Cu (both >99.6% pure, Goodfellow) foils with thicknesses of 10 and 25 μm were irradiated. The beam flux was measured by charge integration as well as via monitor reactions. The cross-sections of the monitor reactions ^{nat}Ti(α,x)^{51}Cr, ^{nat}Cu(α,x)^{66,67}Ga, ^{nat}Cu(α,x)^{65}Zn and ^{nat}Ti(^{3}He,x)^{48}V were taken from an evaluated data file (Tárkányi et al., 2001). The calculation of the energy degradation within each stack was based on the method of Williamson et al. (1966).

2.1.3. Chemical separation procedure

From each irradiated sample at first the thin Al cover foil was removed. The rest of the sample was then subjected to standard γ-ray spectrometry (see Section 2.1.4) and the weak activity of ^{191}Pt ($T_{1/2} = 2.8$ d), formed via the ^{189}Os(α,2n)^{191}Pt and ^{190}Os(α,3n)^{191}Pt reactions on the small amounts of ^{189}Os and ^{190}Os present in the enriched ^{192}Os sample, was determined using a 360 keV γ-ray ($I_\gamma = 6.0\%$). Thereafter, a chemical separation procedure was applied to isolate the radioplatinum from the background activity, thus enabling the preparation of a clean and thin source suitable for X-ray counting. For this purpose, each sample (consisting of about 3 mg osmium and a 25 μm thick Ni foil) was dissolved in about 2 mL of conc. HNO_3 at an elevated temperature of 160 °C. During the dissolution process the enriched osmium was distilled over and recovered (see Section 2.1.6). The remaining solution (containing radioplatinum and the matrix activity) was evaporated to dryness, and the residue redissolved in about 5 mL of 3 M HCl. The next step was the addition of 0.5 mL of a 10% solution of $SnCl_2$ in 3 M HCl. After the reduction of all platinum, the activity was extracted with an equal volume of diethyl- or diisopropylether. This method (Bonardi et al., 1998) was found to be fast and almost quantitative. Prior to its use the ether was brought to a water-free state by treating it with Na_2SO_4. In the organic

phase, no impurities resulting from the dissolved Ni could be observed.

For measuring the activity, the ether phase was transferred to a filter paper and evaporated. This way the X-rays of Pt could be easily measured without much correction for absorption (see Section 2.1.4). Each source was also assayed via γ-ray spectrometry and the activity of ^{191}Pt was redetermined. A comparison of its activity before and after the chemical separation gave the yield of radiochemical separation. It was found to be between 60% and 90%. The γ-ray analysis also showed that the contamination of radioplatinum by non-isotopic radionuclidic impurities (^{56,58}Co, ^{65}Zn, etc.) was $<0.01\%$.

2.1.4. Measurement of radioactivity

For measuring the activity of ^{195m}Pt and ^{193m}Pt in each chemically separated radioplatinum sample, an HPGe detector with a thin Be-window (a special detector for low-energy γ-rays) was used. The sample to detector distance was 3 cm. Spectra were recorded several times to check the half-life of the products. Both the radionuclides were assayed together using 66.8 keV k_α X-rays of Pt. In addition, the 98.9 keV γ-ray ($I_\gamma = 11.4\%$) of ^{195m}Pt was used to determine the activity of this nuclide; the activity of ^{193m}Pt was obtained by subtracting the ^{195m}Pt contribution from the total activity determined via the 66.8 keV X-ray.

For measuring the activity of each monitor foil as well as for determining the radiocontaminants in each radioplatinum sample, standard γ-ray spectrometry using a large-size HPGe detector was applied. The detector was calibrated with standard sources supplied by the Physikalisch-Technische Bundesanstalt and Amersham International. The sample to detector distance was between 10 and 50 cm in the case of monitor foils, and between 3 and 5 cm while measuring the chemically separated radioplatinum samples.

The decay data of the two investigated radionuclides used are given in Table 1 (Firestone, 1996). The count rate of each product was obtained by averaging the results of various measurements extrapolated to the end of bombardment. The absolute activity was then derived by applying the usual corrections like those for γ-ray and X-ray intensity, detector efficiency, etc.

2.1.5. Calculation of cross-section and uncertainty

In order to calculate the beam flux from the beam monitor activity the activation equation was used with the known monitor cross-section data as mentioned above (Tárkányi et al., 2001). With the calculated beam flux and reaction product activity, the cross-section was calculated using again the activation equation. For estimation of uncertainties, see Table 2. The uncertainty in the primary particle energy amounted to 0.2 MeV. The uncertainty in the energy effective at each foil increased with increasing number of foils.

Table 1
Decay properties of the investigated radionuclides[a]

Nuclide	Half-life (d)	Radiation used for activity measurement (keV)	Intensity (%)
^{193m}Pt	4.33	66.8 (Pt $K_{\alpha 1}$ X-ray)	7.4
^{195m}Pt	4.03	66.8 (Pt $K_{\alpha 1}$X-ray)	39.0
		98.9 (γ-ray)	11.4

[a]Taken from Firestone (1996).

Table 2
Uncertainties and their magnitudes in cross-section measurements

Source of uncertainty	Estimated magnitude
Number of target nuclei (%)	2
Target uniformity (%)	5
Chemical yield determination (%)	3
Efficiency of the detector (%)	4–7
Peak area analysis (%)	2–10
Cross-section of monitor reaction (%)	9–12
Decay data (%)	5
Total uncertainty in measured cross-section (%)	12–18
Uncertainty in projectile energy effective in a sample (MeV)	0.2–0.8

2.1.6. Recovery of the enriched material

Recovery of the enriched material was done by dissolution of the thin target and the backing foil in concentrated nitric acid and distillation of the OsO_4 formed into a weak solution of NaOH. The level of radiocontaminants (^{56,58}Co, ^{65}Zn, etc.) in this solution was found to be $<0.01\%$. The solution could thus be used directly for electroplating. The recovery yield was estimated to be $>80\%$.

2.2. Results

2.2.1. $^{192}Os(\alpha,n)^{195m}Pt$ reaction

As mentioned above, the activity of the radiochemically separated ^{195m}Pt was determined using a γ-ray at 98.9 keV and also a K_α X-ray of energy 66.8 keV. Up to about 23 MeV the activity determined via both methods was consistent. At higher energies the X-ray counting gave higher values, whereas the γ-ray analysis gave decreasing values. The threshold of the ^{192}Os(α,3n)^{193m}Pt reaction lies at about 23 MeV. With beam energies above 24 MeV the latter reaction contributes significantly to the emission of X-rays. For the calculation of the cross-section of the ^{192}Os(α,n)^{195m}Pt reaction above 23 MeV, therefore, only the γ-ray was used. The measured cross-sections are given in Table 3 and are graphically shown in Fig. 1. A maximum of about 4 mb at 21.5 MeV can be seen. There are no experimental literature data or results of nuclear model calculations available to compare with.

2.2.2. $^{192}Os(\alpha,3n)^{193m}Pt$ reaction

The K_α X-ray line at 66.8 keV was used to determine the activity of ^{193m}Pt, after subtracting the contribution of

Table 3
Measured cross-sections of the ^{192}Os(α,n)^{195m}Pt and ^{192}Os(α,3n)^{193m}Pt reactions

Particle energy (MeV)	Cross-section (mb)	
	^{192}Os(α,n)^{195m}Pt	^{192}Os(α,3n)^{193m}Pt
27.5±0.2	1.5±0.2	197±30
26.5±0.2	3.3±0.5	129±19
26.3±0.2		160±24
26.0±0.3	1.4±0.2	43±6
25.0±0.3	2.8±0.4	23±4
24.8±0.3		27±4
23.5±0.4	3.3±0.5	7±1
22.1±0.5	4.4±0.7	
21.3±0.5	2.9±0.4	
20.0±0.6	2.4±0.4	
19.2±0.6	3.7±0.6	
18.1±0.7	2.1±0.3	
17.3±0.8	1.7±0.2	
15.9±0.9	0.6±0.1	

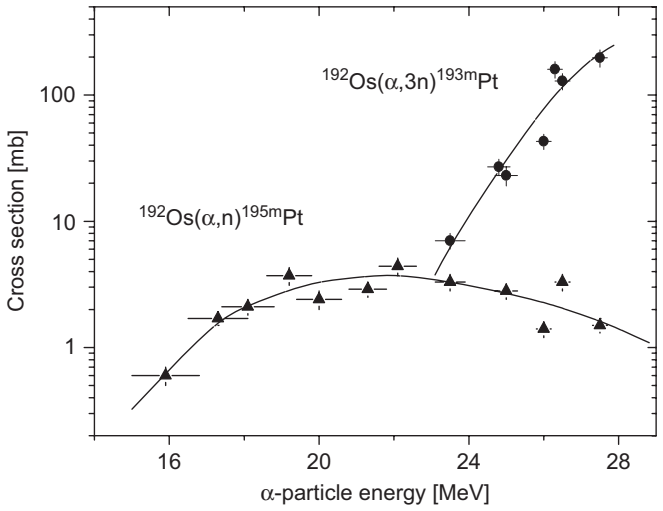

Fig. 1. Experimental cross-section data for the ^{192}Os(α,n)^{195m}Pt and ^{192}Os(α,3n)^{193m}Pt nuclear reactions. The curves act as guides to the eye.

^{195m}Pt. The numerical cross-section values are given in Table 3 and the excitation function in Fig. 1. No maximum was observed in the investigated energy region. Similar to the ^{192}Os(α,n)^{195m}Pt reaction, no literature data were found for comparison.

It should be pointed out that at the α-particle energy of 23.5 MeV, besides the reaction ^{192}Os(α,3n)^{193m}Pt the reaction ^{190}Os(α,n)^{193m}Pt may also contribute to the formation of ^{193m}Pt. However, considering the low abundance of ^{190}Os in the enriched ^{192}Os sample and assuming the cross-section of the ^{190}Os(α,n)-reaction to be similar to that of the ^{192}Os(α,n)-reaction described above, we estimated the contribution of the ^{190}Os(α,n)-reaction to the formation of ^{193m}Pt to be <10% of that of the ^{192}Os(α,3n) process, i.e. within the limits of experimental uncertainties. At energies >24 MeV this contribution becomes negligible.

2.2.3. *Search for the formation of ^{195m}Pt and ^{193m}Pt in ^{3}He-particle-induced reactions on ^{192}Os*

Both ^{195m}Pt and ^{193m}Pt could not be detected in any of the ^{192}Os samples irradiated with ^{3}He-particles. The former would be formed via the (^{3}He,γ) process, the cross-section of which in the medium mass region is known to be extremely small (cf. Carlson and Daly, 1967). The latter radionuclide, however, should be formed via the (^{3}He,2n) process whose cross-section in this mass region is generally not small (Hilgers et al., 2005). Hence, the non-observance of ^{193m}Pt was rather surprising. Probably, the loosely bound ^{3}He-particle cannot efficiently populate the levels with rather high spins.

3. Integral yields

The integrated yields of ^{195m}Pt and ^{193m}Pt in α-particle-induced reactions on ^{192}Os were calculated from the eye-guide excitation curves given in Fig. 1, assuming an irradiation time of 1 h and a particle beam current of 1 μA. The results are shown as a function of projectile energy in Fig. 2. A suitable energy range for the production of ^{195m}Pt seems to be $E_\alpha = 24 \rightarrow 18$ MeV with the calculated ^{195m}Pt yield amounting to about 0.013 MBq/μA h. This yield would increase to 0.019 MBq/μA h if the energy range $E_\alpha = 28 \rightarrow 18$ MeV is used for production. In that case, ^{193m}Pt would also be produced, its yield being 0.25 MBq/μA h in the energy range $E_\alpha = 28 \rightarrow 24$ MeV. Since both these nuclides can be used in the same way and the half-lives are very similar, it may be possible to accept a mixture of the two. For dose calculations, however, it is important to know the activity of both nuclides exactly.

Some comparison of the present results can be done with the experimental yield of the ^{nat}Os(α,xn)^{193m}Pt reaction reported by Tinker et al. (1991). At 38 MeV they could

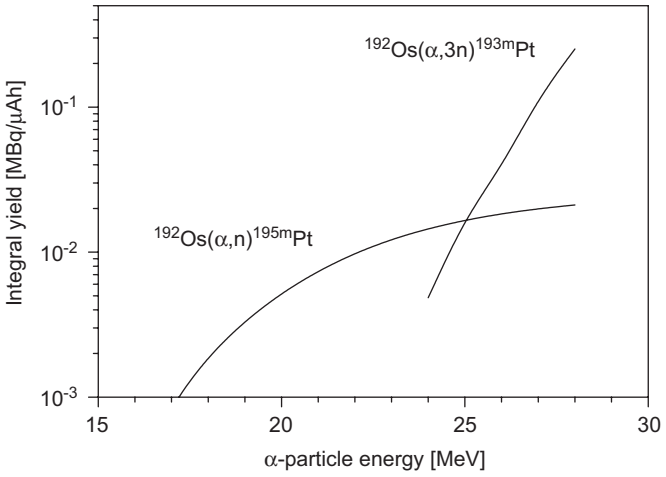

Fig. 2. Integral yields calculated from the excitation functions of the ^{192}Os(α,n)^{195m}Pt and ^{192}Os(α,3n)^{193m}Pt nuclear reactions given in Fig. 1.

achieve 1.1 MBq/μA h of ^{193m}Pt but with considerable contamination from ^{195m}Pt and, above all, ^{191}Pt ($T_{1/2}$ = 2.8 d) which emits hard γ-rays. Since the reaction cross-section of the ^{192}Os(α,3n)^{193m}Pt reaction increases significantly at energies higher than 28 MeV (see Fig. 1), it is predicted that at about 38 MeV the ^{193m}Pt from highly enriched ^{192}Os may reach a value of 6–8 MBq/μA h. This extrapolated value would approximately agree with the yield from ^{nat}Os reported by Tinker et al. (1991). Furthermore, when using an energy range of $E_\alpha = 38 \rightarrow 24$ MeV the contribution of ^{195m}Pt in the mixture of isotopes formed would be negligible. The amount of ^{191}Pt, however, may be significant since it is formed via the (α,3n) reaction on ^{190}Os whose abundance in the enriched ^{192}Os used is not so small.

4. Comparison of reported production routes of ^{195m}Pt and ^{193m}Pt

4.1. Comparison of reactor and cyclotron production of ^{195m}Pt

A comparison of the reactor production data of ^{195m}Pt (Akaboshi, 2003) with the cyclotron production data of the same nuclide reported in this work is given in Table 4. The extrapolated batch yield of ^{195m}Pt in the cyclotron production is about one order of magnitude lower than in the reactor production. However, the specific activity, which is important for internal radiotherapy, ought to be higher in the cyclotron production by two orders of magnitude (see Section 5.5). This method could therefore be of great interest when really high specific activity is needed, although the overall costs would be much higher.

4.2. Comparison of various routes for the production of ^{193m}Pt

The radionuclide ^{193m}Pt can also be produced via reactor neutron irradiation of ^{192}Pt but the highly enriched target material is very expensive due to the low abundance of ^{192}Pt (0.79%). This method has therefore found only limited application for the production of ^{193m}Pt (Azure et al., 1992). A summary of the reactor production data is given in Table 5.

As regards cyclotron production, two methods can be used. In one case, the ^{nat}Ir(d,xn)^{193m}Pt reaction has been suggested. The ^{193m}Pt yield amounts to 5.8 and 9.5 MBq/μA h over the energy ranges $E_d = 19 \rightarrow 14$ MeV and $E_d = 19 \rightarrow 9$ MeV, respectively (Tinker et al., 1991). The radionuclidic purity is, however, low. The other reaction is the ^{192}Os(α,3n)^{193m}Pt process studied in this work. Over the investigated energy range of $E_\alpha = 28 \rightarrow 24$ MeV the ^{193m}Pt yield of 0.25 MBq/μA h is appreciably lower than the yield via the ^{nat}Ir(d,xn)^{193m}Pt process, but the radionuclidic purity is higher.

A comparison of the reactor method of production of ^{193m}Pt with the cyclotron method reported in this work is given in Table 5. The extrapolated batch yield of ^{193m}Pt in the cyclotron production is by about one order of magnitude lower than in the reactor production. However, the specific activity should be about two orders of magnitude higher. Furthermore, the ^{195m}Pt impurity in the cyclotron production of ^{193m}Pt would be much lower than in the reactor production. Additionally, the increasing excitation function of the ^{192}Os(α,3n)^{193m}Pt reaction suggests that the yield of ^{193m}Pt would be much higher if α-particles of energy about 38 MeV would be available. In order to decrease the level of the ^{191}Pt impurity, however, a highly enriched ^{192}Os target would be needed.

Table 4
Comparison of reactor and cyclotron production routes of ^{195m}Pt

Parameter	Production using	
	Nuclear reactor[a]	Cyclotron
Reaction	^{194}Pt (n,γ)^{195m}Pt	^{192}Os(α,n)^{195m}Pt
Cross-section	$\langle\sigma\rangle = 0.09$ b	$\sigma_{max} = 3.7$ mb
Target enrichment	95%	84.5%
Flux	8.15×10^{13} n/cm^2/s	9.36×10^{14} α/s[c]
Irradiation time	75 h	30 h
Yield	1 GBq	0.09 GBq
Specific activity[b]	11 GBq/g Pt	n.c.a

[a]Data reported by Akaboshi (2003).
[b]At ORNL, a 97.4% enriched ^{194}Pt target irradiated at a flux of 2.5×10^{15} n/cm^2/s for 36 h led to a specific activity of 44 GBq ^{195m}Pt/g Pt (Hoeschele et al., 1982).
[c]Assuming a beam current of 300 μA.

Table 5
Comparison of reactor and cyclotron production routes of ^{193m}Pt

Parameter	Production using	
	Nuclear reactor[a]	Cyclotron
Reaction	^{192}Pt(n,γ)^{193m}Pt	^{192}Os(α,3n)^{193m}Pt
Cross-section	$\langle\sigma\rangle = 2$ b	$\sigma_{27.5\,MeV} = 197$ mb
Target enrichment	57%	84.5%
Flux	4×10^{14} n/cm^2/s	9.36×10^{14} α/s[b]
Irradiation time	7 d	30 h
Batch yield	ca. 3 GBq	0.225 GBq[c]
Impurity	^{195m}Pt (12%)	^{195m}Pt (<2%); ^{191}Pt (<15%)[d]

[a]Data reported by Azure et al. (1992).
[b]Assuming a beam current of 300 μA.
[c]Batch yield would be considerably higher with α-particles with an energy of 38 MeV.
[d]The level of this impurity could be considerably reduced by using highly enriched ^{192}Os as the target material.

5. High-current production tests

5.1. Sample preparation

Samples for high-current irradiations for the production of ^{195m}Pt and ^{193m}Pt were prepared electrolytically as described in the section on cross-section data. Increased

target thicknesses could be achieved by performing the electrolysis up to ten cycles. In this case, 1 mm thick Ni- or stainless-steel plates of 25 mm diameter (see below) were used as backings, but the diameter of the actual ^{192}Os layer was 14 mm.

5.2. High current irradiations

A slanting beam target system developed in our institute for the production of ^{124}I was used for high current irradiations of ^{192}Os samples. The target holder consisted of a cooling body made of brass. The cooling body had a circular hole through which it was connected to a pipe for cooling water. The Ni- or stainless-steel plate mentioned above was fixed above the circular hole. The back of the plate was thus cooled directly by flowing water, which was very efficient. Irradiations were done with 28 MeV α-particle beam currents of up to 20 μA at an angle of 20°. The dissipated power density was estimated to be 60 W/cm^2.

5.3. Chemical separation

Owing to the rather thick target backing used in production tests, and because of the higher quality product needed for medical application, the radiochemical separation procedure developed was somewhat different from that used in nuclear data measurements (described in Section 2.1.3). The first step here was the dissolution of parts of the backing with concentrated hydrochloric acid. Thereby osmium remained in metal form. This metal was washed alternatively with water and hydrochloric acid four times to remove the radionuclides from the nickel backing (mainly ^{56,58}Co and ^{65}Zn). After the number of these nuclides had decreased to a reasonably low level, osmium was dissolved in concentrated nitric acid. The OsO_4 formed was distilled over to an alkaline solution and could be reused. The rest of the disturbing radionuclides were separated from the radioplatinum via cation-exchange chromatography using Dowex 50WX8 as the resin and hydrochloric acid as the eluting agent (cf. Bonardi et al., 1998). The radiochemical yield of the radioplatinum separation process at the no-carrier-added level was estimated to lie between 50% and 90%. The level of the non-isotopic radionuclidic impurities was very low (see below).

5.4. Comparison of calculated and experimental batch yields of ^{195m}Pt and ^{193m}Pt

A comparison of the experimental and theoretical batch yields, calculated from the excitation functions (see above), is given in Table 6. As can be seen, the experimental yield amounts to between 25% and 90% of the respective theoretical value. The difference was large when a thin target was used, possibly due to a large uncertainty in the calculated energy range. In case of thicker targets, the lower experimental values are possibly due to inhomogeneities inside the target, non-homogenuos beam-profiling, radiation damage effects, losses in chemical processing, etc. (Qaim, 1989). The highest experimental batch yield of ^{195m}Pt achieved was about 1 MBq (with about 55% ^{193m}Pt and 5% ^{191}Pt as impurity) and of ^{193m}Pt about 9 MBq (with 4% ^{195m}Pt and 10% ^{191}Pt as impurity). Thus, it is possible to produce relatively pure ^{193m}Pt. The amount of ^{191}Pt could be considerably reduced by using highly enriched ^{192}Os as a target material. For obtaining pure ^{195m}Pt, on the other hand, the α-particle energy region <23 MeV will have to be utilized, resulting in some reduction in its yield.

5.5. Quality control

The separated platinum nuclides were checked for their quality as follows:

- The radionuclidic purity was checked using HPGe detectors. In all cases, no or only small contamination from ^{56,58}Co or ^{65}Zn (0.01%) was found. The ^{193m}Pt produced using the energy range $E_\alpha = 28 \rightarrow 22.3$ MeV contained 4% ^{195m}Pt and about 10% ^{191}Pt.
- The radiochemical quality was checked via the behaviour of the radioplatinum on the cation-exchange column using published methods (cf. Bonardi et al., 1998).
- The chemical purity was checked via ICP-MS analysis. All chemical contaminations were in the order of a few μg/L.

Table 6
Comparison of experimental and calculated yields of ^{195m}Pt and ^{193m}Pt

Energy range of α-particles (MeV)	Beam current (μA)	Irradiation time (h)	^{195m}Pt batch yield (MBq)		^{193m}Pt batch yield (MBq)	
			Calculated	Experimental	Calculated	Experimental
28→25.3	9.9	5.9	0.16	0.1	5.49	2.1
28→25.5	19.1	6.6	0.35	0.2	11.6	4.8
28→26.7	21.1	6.2	0.28	0.07	4.8	1.7
28→27.0	21.5	5.4	0.3	0.2	11.0	2.6
28→22.3	19.3	4.9	0.37	0.3	9.7	8.7
25.4→18.2	14.8	11.2	1.3	0.9	0.9	0.5

- The amount of Pt in the separated product was also checked via ICP-MS. The specific activity of ^{195m}Pt was estimated as 1 TBq/g Pt and that of ^{193m}Pt as 9 TBq/g Pt. These values can be improved, e.g. by avoiding the Pt anode in the electrolytic sample preparation, by increasing the beam current and the irradiation time and, in case of ^{193m}Pt, by increasing the α-particle energy.

6. Conclusions

The interaction of ^{3}He particles with ^{192}Os produces neither ^{195m}Pt nor ^{193m}Pt. New cross-section data for the nuclear reactions ^{192}Os(α,n)^{195m}Pt and ^{192}Os(α,3n)^{193m}Pt could be achieved. A production method for platinum radionuclides from α-particle irradiation of ^{192}Os was developed. The yields of ^{195m}Pt and ^{193m}Pt in cyclotron production are much lower than those in reactor production but the specific activity in both cases is higher by two orders of magnitude. The yield of ^{193m}Pt could be considerably increased if α-particles of energy about 38 MeV would be available.

Acknowledgements

We thank the operators of the compact cyclotron CV 28 at Jülich for performing the irradiations, Mr. S. Spellerberg and Mr. W. Bolten for technical assistance, and the Zentralabteilung für Chemische Analysen (ZCH) for checking inactive chemical impurities in the separated radioplatinum via ICP-MS analysis.

References

Akaboshi, M., 2003. Platinum 195 m: in manual for reactor produced radioisotopes. IAEA-TECDOC-1340, pp. 171–178.

Azure, M.T., Sastry, K.S.R., Archer, R.D., Howell, R.W., Rao, D.V., 1992. Micorscale synthesis of carboplatin labelled with the Auger emitter ^{193m}Pt: radiotoxicity versus chemotoxicity of the antitumor drug in mammalian cells. In: Howell, R.W., Narra, V.R., Sastry, K.S.R., Rao, D.V. (Eds.), Biophysical Aspects of Auger Processes. American Institute of Physics, Inc., Woodbury, NY 11797, USA, pp. 336–351.

Bonardi, M., Birattari, C., Gallorini, M., Groppi, F., Arginelli, D., Gini, L., 1998. Cyclotoron production, radiochemical separation and quality control of platinum radiotracers for toxicological studies. J. Radioanal. Nucl. Chem. 236, 159–164.

Carlson, R.V., Daly, P.J., 1967. Excitation functions of (^{3}He,γ) and (^{4}He,γ) reactions. Nucl. Phys. A 102, 161.

Chakrabarty, S., Tomar, B.S., Goswani, A., Raman, V.A., Manohar, S.B., 2001. Preparation of thin osmium targets by electrodeposition. Nucl. Instrum. Methods B 174, 212–216.

Fresenius, W., Jander, G., 1951. Handbuch der analytischen Chemie, Zweiter Teil: qualitative Nachweisverfahren, Band VIII b β Elemente der achten Hauptgruppe, II (Platinmetalle). Springer OHG, Berlin, Göttingen, Heidelberg, Germany, p. 172.

Firestone, R.B., 1996. Tables of Isotopes, CDROM-Edition, Version 1.0. Wiley-Interscience, New York.

Groppi, F., Birattari, C., Bonardi, M., Gallorini, M., Gini, L., 2001. Thin target excitation functions for (α,xn) reactions on osmium targets for platinum radiotracer production. J. Radioanal. Nucl. Chem. 249, 289–293.

Hilgers, K., Shubin, Yu.N., Coenen, H.H., Qaim, S.M., 2005. Experimental measurements and nuclear model calculations on the excitation functions of ^{nat}Ce(^{3}He,xn) and ^{141}Pr(p,xn) reactions with special reference to production of the therapeutic radionuclide ^{140}Nd. Radiochim. Acta 93, 553–560.

Hoefnagel, C.A., 1991. Radionuclide therapy revisited. Eur. J. Nucl. Med. 18, 408–431.

Hoeschele, J.D., Butler, T.A., Roberts, J.A., Guyer, C.E., 1982. Analysis and refinement of the microscale synthesis of the ^{195m}Pt-labelled antitumor drug, *cis*-dichlorodiammineplatinum(II), *cis*-DDP. Radiochim. Acta 31, 27–36.

Mariani, G., Bodei, L., Adelstein, S.J., Kassis, A.I., 2000. Emerging roles for radiometabolic therapy of tumors based on Auger electron emission. J. Nucl. Med. 41, 1519–1521.

Mushtaq, A., Qaim, S.M., 1990. Excitation functions of alpha- and ^{3}He-particle induced nuclear reactions on natural germanium: evaluation of production routes for ^{73}Se. Radiochim. Acta 50, 27–31.

Qaim, S.M., 1989. Target development for medical radioisotope production at a cyclotron. Nucl. Instrum. Methods A 282, 289–295.

Qaim, S.M., 2001. Therapeutic radionuclies and nuclear data. Radiochim. Acta 89, 297–302.

Tárkányi, T.F., Gul, K., Hermanne, A., Mustafa, M.G., Nortier, F.M., Qaim, S.M., Scholten, B., Shubin, Yu., Takács, S., Zhuang, Y., 2001. Beam monitor reactions: in charged-particle cross section database for medical radioisotope production. IAEA-TECDOC-1211, pp. 49–152.

Tinker, N.D., Zweit, J., Sharma, H.L., Downey, S., McAuliffe, C.A., 1991. Production of no-carrier added ^{191}Pt, a radiolabel for the synthesis and biological investigations of platinum anti-tumor compounds. Radiochim. Acta 54, 29–34.

Williamson, C.F., Boujot, J.P., Picard, J., 1966. Tables of range and stopping power of chemical elements for charged particles of energies from 0.5 to 500 MeV. Rapport CEA-R 3042.